

Free vibration analysis of spherical caps by the pseudospectral method[†]

Jinhee Lee^{*}

Department of Mechano-Informatics, Hongik University, Choongnam, 339-701, Korea

(Manuscript Received July 28, 2008; Revised September 5, 2008; Accepted September 7, 2008)

Abstract

The pseudospectral method is applied to the axisymmetric and asymmetric free vibration analysis of spherical caps. The displacements and the rotations are expressed by Chebyshev polynomials and Fourier series, and the collocated equations of motion are obtained in terms of the circumferential wave number. Numerical examples are provided for clamped, hinged and free boundary conditions. The results show good agreement with those of existing literature.

Keywords: Chebyshev polynomials; Free vibration; Pseudospectral method; Spherical shell

1. Introduction

Research on the free vibration of spherical caps can largely be divided into two groups: the analytical approach and the application of the discretization methods. Hoppmann [1] proposed employing Bessel functions in the analysis of axisymmetric free vibration of shallow spherical shells. Legendre functions were widely used in the axisymmetric free vibration analyses of spherical caps [2-4]. Prasad [5] obtained the solution of the reduced equations of motion of spherical caps by the use of associated Legendre functions. Zarghamee and Robinson [6] applied the Holzer method to the axisymmetric and asymmetric free vibration analysis of clamped spherical caps. Wu and Heyliger [7] approximated the axisymmetric and asymmetric modes of spherical cap vibrations by Hermite polynomials and Fourier series.

The finite element method has been one of the most favored discretization methods in the vibration analyses of spherical shells. Singh and Mirza [8] applied it to the analysis of the asymmetric vibration of spherical caps where clamped and hinged boundary condi-

tions were considered. Tessler and Spiridigliozzi [9] developed a two-node axisymmetric shell element to compute the natural frequencies of clamped hemispherical shells. Gautham and Ganesan [10] studied the axisymmetric and asymmetric free vibrations of clamped spherical caps using shear deformable semi-analytic shell finite elements. Buchanan and Rich [11] computed the natural frequencies of spherical shells with simply supported, free and fixed boundary conditions using a Lagrangian finite element in spherical coordinates. Fan and Luah [12] used the spline finite element method to compute the natural frequencies of clamped hemispherical domes.

In this study, the pseudospectral method is applied to the symmetric and asymmetric modes of free vibration analysis of spherical caps, where Chebyshev polynomials and Fourier series are selected as the basis functions in the colatitudinal direction and in the circumferential direction, respectively. The pseudospectral method can be considered to be a spectral method that performs a collocation process. A brief explanation of the pseudospectral method can be found in the free vibration analysis of helical springs [13].

2. Pseudospectral formulations

The equations of motion of spherical shells with the

[†] This paper was recommended for publication in revised form by Associate Editor Eung-Soo Shin

^{*} Corresponding author. +82 41 860 2589, Fax.: +82 41 862 2664

E-mail address: jinheelee@hongik.ac.kr

© KSME & Springer 2009

effects of transverse shear and rotary inertia taken into account were derived by Soedel [14] as

$$\frac{\partial}{\partial \phi} (N_\phi \sin \phi) + \frac{\partial N_{\phi\theta}}{\partial \theta} - N_\theta \cos \phi + Q_\phi \sin \phi = -\omega^2 R \sin \phi \rho h U, \tag{1a}$$

$$\frac{\partial}{\partial \phi} (N_{\phi\theta} \sin \phi) + \frac{\partial N_\theta}{\partial \theta} + N_{\phi\theta} \cos \phi + Q_\theta \sin \phi = -\omega^2 R \sin \phi \rho h V, \tag{1b}$$

$$\frac{\partial}{\partial \phi} (Q_\phi \sin \phi) + \frac{\partial Q_\theta}{\partial \theta} - (N_\phi + N_\theta) \sin \phi = -\omega^2 R \sin \phi \rho h W, \tag{1c}$$

$$\frac{\partial}{\partial \phi} (M_\phi \sin \phi) + \frac{\partial M_{\phi\theta}}{\partial \theta} - M_\theta \cos \phi - Q_\phi R \sin \phi = -\omega^2 R \sin \phi \frac{\rho h^3}{12} \Psi_\phi, \tag{1d}$$

$$\frac{\partial}{\partial \phi} (M_{\phi\theta} \sin \phi) + \frac{\partial M_\theta}{\partial \theta} + M_{\phi\theta} \cos \phi - Q_\theta R \sin \phi = -\omega^2 R \sin \phi \frac{\rho h^3}{12} \Psi_\theta, \tag{1e}$$

for harmonic motions at natural frequency ω in radian/second. U , V and W are the displacements in the colatitudinal, circumferential and normal directions, respectively, as shown in Fig. 1. Ψ_ϕ and Ψ_θ are the rotations in the colatitudinal and circumferential directions. R , h and ρ are the radius, the wall thickness and the density of the spherical shell. Φ is the spherical cap angle.

The stress resultants N_ϕ , N_θ , $N_{\phi\theta}$, Q_ϕ , Q_θ , M_ϕ , M_θ and $M_{\phi\theta}$ are defined as

$$N_\phi = C \left\{ \frac{1}{R} \frac{\partial U}{\partial \phi} + \frac{W}{R} + v \left(\frac{1}{R \sin \phi} \frac{\partial V}{\partial \theta} + \frac{U}{R \tan \phi} + \frac{W}{R} \right) \right\}, \tag{2a}$$

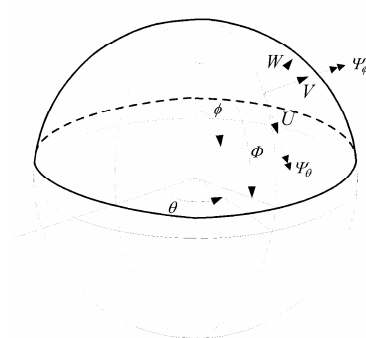


Fig. 1. Geometry of a spherical cap.

$$N_\theta = C \left\{ \frac{1}{R \sin \phi} \frac{\partial V}{\partial \theta} + \frac{U}{R \tan \phi} + \frac{W}{R} + v \left(\frac{1}{R} \frac{\partial U}{\partial \phi} + \frac{W}{R} \right) \right\}, \tag{2b}$$

$$N_{\phi\theta} = N_{\theta\phi} = \frac{1-v}{2} C \left(\frac{1}{R} \frac{\partial V}{\partial \theta} - \frac{V}{R \tan \phi} + \frac{1}{R \sin \phi} \frac{\partial U}{\partial \theta} \right), \tag{2c}$$

$$M_\phi = D \left\{ \frac{1}{R} \frac{\partial \Psi_\phi}{\partial \phi} + v \left(\frac{1}{R \sin \phi} \frac{\partial \Psi_\theta}{\partial \theta} + \frac{\Psi_\theta}{R \tan \phi} \right) \right\}, \tag{2d}$$

$$M_\theta = D \left(\frac{1}{R \sin \phi} \frac{\partial \Psi_\theta}{\partial \theta} + \frac{\Psi_\theta}{R \tan \phi} + \frac{v}{R} \frac{\partial \Psi_\phi}{\partial \phi} \right), \tag{2e}$$

$$M_{\phi\theta} = M_{\theta\phi} = \frac{1-v}{2} D \left(\frac{1}{R} \frac{\partial \Psi_\theta}{\partial \theta} - \frac{\Psi_\theta}{R \tan \phi} + \frac{1}{R \sin \phi} \frac{\partial \Psi_\phi}{\partial \theta} \right), \tag{2f}$$

$$Q_\phi = \kappa Gh \left(\Psi_\phi - \frac{U}{R} + \frac{1}{R} \frac{\partial W}{\partial \phi} \right), \tag{2g}$$

$$Q_\theta = \kappa Gh \left(\Psi_\theta - \frac{V}{R} + \frac{1}{R \sin \phi} \frac{\partial W}{\partial \theta} \right). \tag{2h}$$

C and D are defined as $C = Eh / (1 - \nu^2)$ and $D = Eh^3 / 12(1 - \nu^2)$. E , G , ν and κ represent Young's modulus, the shear modulus, Poisson's ratio and the shear correction factor, respectively.

When the stress resultants of Eqs. (2a)-(2h) are substituted into the equations of motion (1a)-(1e) we have

$$\sin \phi \frac{\partial^2 U}{\partial \phi^2} + \cos \phi \frac{\partial U}{\partial \phi} + \frac{1-\nu}{2 \sin \phi} \frac{\partial^2 U}{\partial \theta^2} - \left(\frac{1}{\tan^2 \phi} + \nu + \frac{\kappa Gh}{C} \right) \sin \phi U + \frac{1+\nu}{2} \frac{\partial^2 V}{\partial \phi \partial \theta} - \frac{3-\nu}{2 \tan \phi} \frac{\partial V}{\partial \theta} + \left(1 + \nu + \frac{\kappa Gh}{C} \right) \sin \phi \frac{\partial W}{\partial \phi} + \frac{\kappa Gh}{C} R \sin \phi \Psi_\phi = -\omega^2 R^2 \sin \phi \frac{\rho h}{C} U, \tag{3a}$$

$$\begin{aligned} & \frac{1+\nu}{2} \frac{\partial^2 U}{\partial \phi \partial \theta} + \frac{3-\nu}{2 \tan \phi} \frac{\partial U}{\partial \theta} + \frac{1-\nu}{2} \left(\sin \phi \frac{\partial^2 V}{\partial \phi^2} + \cos \phi \frac{\partial V}{\partial \phi} \right) + \frac{1}{\sin \phi} \frac{\partial^2 V}{\partial \theta^2} \\ & - \left\{ \frac{1-\nu}{2} \left(\frac{1}{\tan^2 \phi} - 1 \right) + \frac{\kappa Gh}{C} \right\} \sin \phi V \\ & + \left(1 + \nu + \frac{\kappa Gh}{C} \right) \frac{\partial W}{\partial \theta} + \frac{\kappa Gh}{C} R \sin \phi \Psi_\theta \\ & = -\omega^2 R^2 \sin \phi \frac{\rho h}{C} V, \end{aligned} \tag{3b}$$

$$\begin{aligned}
 & -\left(1+\nu+\frac{\kappa Gh}{C}\right)\left(\sin\phi\frac{\partial U}{\partial\phi}+\cos\phi U+\frac{\partial V}{\partial\theta}\right) \\
 & +\frac{\kappa Gh}{C}\left(\sin\phi\frac{\partial^2 W}{\partial\phi^2}+\cos\phi\frac{\partial W}{\partial\phi}+\frac{1}{\sin\phi}\frac{\partial^2 W}{\partial\theta^2}\right) \\
 & -2(1+\nu)\sin\phi W \\
 & +\frac{\kappa Gh}{C}R\left(\sin\phi\frac{\partial\Psi_\phi}{\partial\phi}+\cos\phi\Psi_\phi+\frac{\partial\Psi_\theta}{\partial\theta}\right) \\
 & =-\omega^2 R^2\sin\phi\frac{\rho h}{C}W,
 \end{aligned}
 \tag{3c}$$

$$\begin{aligned}
 & \frac{\kappa Gh}{D}R\sin\phi\left(U-\frac{\partial W}{\partial\phi}\right)+\sin\phi\frac{\partial^2\Psi_\phi}{\partial\phi^2}+\cos\phi\frac{\partial\Psi_\phi}{\partial\phi} \\
 & +\frac{1-\nu}{2\sin\phi}\frac{\partial^2\Psi_\phi}{\partial\theta^2}-\left(\frac{1}{\tan^2\phi}+\nu+\frac{\kappa Gh}{D}R^2\right)\sin\phi\Psi_\phi
 \end{aligned}
 \tag{3d}$$

$$\begin{aligned}
 & +\frac{1+\nu}{2}\frac{\partial^2\Psi_\theta}{\partial\phi\partial\theta}-\frac{3-\nu}{2\tan\phi}\frac{\partial\Psi_\theta}{\partial\theta}=-\omega^2 R^2\sin\phi\frac{\rho h^3}{12D}\Psi_\phi, \\
 & \frac{\kappa Gh}{D}R\left(\sin\phi V-\frac{\partial W}{\partial\theta}\right)+\frac{1+\nu}{2}\frac{\partial^2\Psi_\phi}{\partial\phi\partial\theta}+\frac{3-\nu}{2\tan\phi}\frac{\partial\Psi_\phi}{\partial\theta} \\
 & +\frac{1-\nu}{2}\left(\sin\phi\frac{\partial^2\Psi_\theta}{\partial\phi^2}+\cos\phi\frac{\partial\Psi_\theta}{\partial\phi}\right)+\frac{1}{\sin\phi}\frac{\partial^2\Psi_\theta}{\partial\theta^2} \\
 & -\left\{\frac{1-\nu}{2}\left(\frac{1}{\tan^2\phi}-1\right)+\frac{\kappa Gh}{D}R^2\right\}\sin\phi\Psi_\theta \\
 & =-\omega^2 R^2\sin\phi\frac{\rho h^3}{12D}\Psi_\theta.
 \end{aligned}
 \tag{3e}$$

Typical boundary conditions are clamped:

$$U=0, V=0, W=0, \Psi_\phi=0, \Psi_\theta=0, \tag{4a}$$

hinged:

$$U=0, V=0, W=0, \Psi_\theta=0, M_\phi=0, \tag{4b}$$

free:

$$N_\phi=0, N_{\phi\theta}=0, Q_\phi=0, M_\phi=0, M_{\phi\theta}=0. \tag{4c}$$

Assume a function $f(\phi, \theta)$ which is periodic in the circumferential direction

$$f(\phi, \theta) = \sum_{n=0}^{\infty} f_n(\phi) \cos n\theta \tag{5}$$

and follow the term $f_n(\phi) \cos n\theta$ along a meridian over the pole. The polar projection of Fig. 2(a) shows

that the component $f_n(\phi)$ does not change sign as the pole is crossed when n is even, while Fig. 2 (b) indicates that $f_n(\phi)$ must always change sign as the pole is crossed when n is odd. Fig. 2 (a) and Fig. 2 (b) imply that $f_n(\phi)$ is an odd function when n is an odd number and that $f_n(\phi)$ is an even function when n is an even number.

The Chebyshev polynomials of the first kind are defined recursively as

$$\begin{cases} T_0(x) = 1, \\ T_1(x) = x, \\ T_k(x) = 2xT_{k-1}(x) - T_{k-2}(x) \quad (k \geq 2) \end{cases} \quad (-1 \leq x \leq 1) \tag{6}$$

which makes the terms $T_0(x), T_2(x), T_4(x), \dots$ be even functions of x , while $T_1(x), T_3(x), T_5(x), \dots$ are odd functions of x .

The colatitude ϕ ranges from 0 to Φ , and it is convenient to use the normalized form

$$\xi = \frac{\phi}{\Phi} \in [0, 1]. \tag{7}$$

The displacements and the rotations are then approximated as follows:

$$U(\xi, \theta) = \sum_{k=1}^{K+1} a_k F_k(\xi) \cos n\theta, \tag{8a}$$

$$V(\xi, \theta) = \sum_{k=1}^{K+1} b_k F_k(\xi) \sin n\theta, \tag{8b}$$

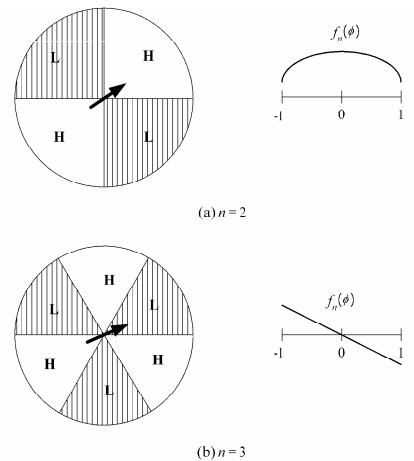


Fig. 2. Polar projections in the vicinity of the pole showing the positive (H) and negative (L) regions for a term $f_n(\phi) \cos n\theta$.

$$W(\xi, \theta) = \sum_{k=1}^{K+1} c_k F_k(\xi) \cos n\theta, \tag{8c}$$

$$\Psi_\phi(\xi, \theta) = \sum_{k=1}^{K+1} d_k F_k(\xi) \cos n\theta, \tag{8d}$$

$$\Psi_\theta(\xi, \theta) = \sum_{k=1}^{K+1} e_k F_k(\xi) \sin n\theta, \tag{8e}$$

where a_k, b_k, c_k, d_k and e_k are the expansion coefficients. K is the number of collocation points in the colatitudinal direction. $F_k(\xi)$ is the basis function selected to be an odd function for odd n , and an even function for even n . Such a basis function can be realized by use of Chebyshev polynomials as follows:

$$F_k(\xi) = \begin{cases} T_{2k-2}(\xi) & (n = 0, 2, 4, \dots), \\ T_{2k-1}(\xi) & (n = 1, 3, 5, \dots). \end{cases} \tag{9}$$

Expansions of (8a)-(8e) are substituted into Eqs. (3a)-(3e), which are then collocated at the Gauss-Lobatto collocation points,

$$\xi_i = \cos \frac{\pi(2i-1)}{4K} \quad (i = 1, 2, \dots, K) \tag{10}$$

to yield the collocated equations as follows:

$$\begin{aligned} & \sum_{k=1}^{K+1} a_k \left[\frac{\sin \phi_i}{\Phi^2} F_k''(\xi_i) + \frac{\cos \phi_i}{\Phi} F_k'(\xi_i) \right. \\ & \left. - \left\{ \frac{(1-\nu)n^2}{2\sin^2 \phi_i} + \frac{1}{\tan^2 \phi_i} + \nu + \frac{\kappa Gh}{C} \right\} \sin \phi_i F_k(\xi_i) \right] \\ & + \sum_{k=1}^{K+1} b_k \left\{ \frac{(1+\nu)n}{2\Phi} F_k'(\xi_i) - \frac{(3-\nu)n}{2\tan \phi_i} F_k(\xi_i) \right\} \\ & + \sum_{k=1}^{K+1} c_k \left(1 + \nu + \frac{\kappa Gh}{C} \right) \frac{\sin \phi_i}{\Phi} F_k'(\xi_i) \\ & + \sum_{k=1}^{K+1} d_k \frac{\kappa Gh}{C} R \sin \phi_i F_k(\xi_i) \\ & = -\omega^2 \sum_{k=1}^{K+1} a_k \frac{R^2 \sin \phi_i \rho h}{C} F_k(\xi_i), \end{aligned} \tag{11a}$$

$$\begin{aligned} & - \sum_{k=1}^{K+1} a_k \left\{ \frac{(1+\nu)n}{2\Phi} F_k'(\xi_i) + \frac{(3-\nu)n}{2\tan \phi_i} F_k(\xi_i) \right\} \\ & - \sum_{k=1}^{K+1} c_k n \left(1 + \nu + \frac{\kappa Gh}{C} \right) F_k(\xi_i) \\ & + \sum_{k=1}^{K+1} b_k \left[\frac{(1-\nu)\sin \phi_i}{2\Phi^2} F_k''(\xi_i) + \frac{(1-\nu)\cos \phi_i}{2\Phi} F_k'(\xi_i) \right. \\ & \left. - \left\{ \frac{n^2}{\sin^2 \phi_i} + \frac{1-\nu}{2} \left(\frac{1}{\tan^2 \phi_i} - 1 \right) + \frac{\kappa Gh}{C} \right\} \sin \phi_i F_k(\xi_i) \right] \\ & + \sum_{k=1}^{K+1} e_k \frac{\kappa Gh}{C} R \sin \phi_i F_k(\xi_i) \\ & = -\omega^2 \sum_{k=1}^{K+1} b_k \frac{R^2 \sin \phi_i \rho h}{C} F_k(\xi_i), \end{aligned} \tag{11b}$$

$$\begin{aligned} & - \sum_{k=1}^{K+1} a_k \left(1 + \nu + \frac{\kappa Gh}{C} \right) \left\{ \frac{\sin \phi_i}{\Phi} F_k'(\xi_i) + \cos \phi_i F_k(\xi_i) \right\} \\ & - \sum_{k=1}^{K+1} b_k n \left(1 + \nu + \frac{\kappa Gh}{C} \right) F_k(\xi_i) \\ & + \sum_{k=1}^{K+1} c_k \left[\frac{\kappa Gh \sin \phi_i}{C \Phi^2} F_k''(\xi_i) + \frac{\kappa Gh \cos \phi_i}{C \Phi} F_k'(\xi_i) \right. \\ & \left. - \left\{ \frac{\kappa Gh}{C} \frac{n^2}{\sin \phi_i} + 2(1+\nu) \sin \phi_i \right\} F_k(\xi_i) \right] \end{aligned} \tag{11c}$$

$$\begin{aligned} & + \sum_{k=1}^{K+1} d_k \frac{\kappa Gh}{C} R \left\{ \frac{\sin \phi_i}{\Phi} F_k'(\xi_i) + \cos \phi_i F_k(\xi_i) \right\} \\ & + \sum_{k=1}^{K+1} e_k n \frac{\kappa Gh}{C} R F_k(\xi_i) \\ & = -\omega^2 \sum_{k=1}^{K+1} c_k \frac{R^2 \sin \phi_i \rho h}{C} F_k(\xi_i), \\ & \sum_{k=1}^{K+1} a_k \frac{\kappa Gh}{D} R \sin \phi_i F_k(\xi_i) - \sum_{k=1}^{K+1} c_k \frac{\kappa Gh}{D} \frac{R \sin \phi_i}{\Phi} F_k'(\xi_i) \\ & + \sum_{k=1}^{K+1} d_k \left[\frac{\sin \phi_i}{\Phi^2} F_k''(\xi_i) + \frac{\cos \phi_i}{\Phi} F_k'(\xi_i) \right. \\ & \left. - \left\{ \frac{(1-\nu)n^2}{2\sin^2 \phi_i} + \frac{1}{\tan^2 \phi_i} + \nu + \frac{\kappa Gh}{D} R^2 \right\} \sin \phi_i F_k(\xi_i) \right] \end{aligned} \tag{11d}$$

$$\begin{aligned} & + \sum_{k=1}^{K+1} e_k \left\{ \frac{(1+\nu)n}{2\Phi} F_k'(\xi_i) - \frac{(3-\nu)n}{2\tan \phi_i} F_k(\xi_i) \right\} \\ & = -\omega^2 \sum_{k=1}^{K+1} d_k \frac{R^2 \sin \phi_i \rho h^3}{12D} F_k(\xi_i), \\ & \sum_{k=1}^{K+1} b_k \frac{\kappa Gh}{D} R \sin \phi_i F_k(\xi_i) + \sum_{k=1}^{K+1} c_k \frac{\kappa Gh}{D} R n F_k(\xi_i) \\ & - \sum_{k=1}^{K+1} d_k \left\{ \frac{(1+\nu)n}{2\Phi} F_k'(\xi_i) + \frac{(3-\nu)n}{2\tan \phi_i} F_k(\xi_i) \right\} \\ & + \sum_{k=1}^{K+1} e_k \left[\frac{(1-\nu)\sin \phi_i}{2\Phi^2} F_k''(\xi_i) + \frac{(1-\nu)\cos \phi_i}{2\Phi} F_k'(\xi_i) \right. \end{aligned} \tag{11e}$$

$$\begin{aligned} & \left. - \left\{ \frac{n^2}{\sin^2 \phi_i} + \frac{1-\nu}{2} \left(\frac{1}{\tan^2 \phi_i} - 1 \right) + \frac{\kappa Gh}{D} R^2 \right\} \sin \phi_i F_k(\xi_i) \right] \\ & = -\omega^2 \sum_{k=1}^{K+1} e_k \frac{R^2 \sin \phi_i \rho h^3}{12D} F_k(\xi_i), \\ & (i = 1, 2, \dots, K) \end{aligned}$$

with $\phi_i = \Phi \xi_i$. The notation (\cdot) stands for the differentiation with respect to ξ . Eqs. (11a-e) are rearranged as

$$[\mathbf{A}(n)]\{\delta\} + [\mathbf{B}(n)]\{\chi\} = \omega^2 ([\mathbf{C}(n)]\{\delta\} + [\mathbf{D}(n)]\{\chi\}) \tag{12}$$

where matrices $[\mathbf{A}(n)], [\mathbf{B}(n)], [\mathbf{C}(n)]$ and $[\mathbf{D}(n)]$ correspond to the circumferential wave number n . The vectors in Eq. (12) are defined as

$$\begin{aligned} \{\delta\} &= \{a_1 \ a_2 \ \dots \ a_K \ b_1 \ b_2 \ \dots \ b_K \ c_1 \ c_2 \ \dots \ c_K \\ & \ d_1 \ d_2 \ \dots \ d_K \ e_1 \ e_2 \ \dots \ e_K\}^T, \\ \{\chi\} &= \{a_{K+1} \ b_{K+1} \ c_{K+1} \ d_{K+1} \ e_{K+1}\}^T. \end{aligned} \tag{13}$$

The total number of equations in Eqs. (11a)-(11e) is $5K$, whereas the total number of expansion coefficients is $5(K+1)$. The remaining five equations are obtained from the boundary conditions. The boundary conditions (4a)-(4c) at $\xi = 1$ are expressed by use of the expansions of Eqs. (8a)-(8e) as follows:

clamped:

$$\left\{ \begin{aligned} \sum_{k=1}^{K+1} a_k F_k(1) = 0, \quad \sum_{k=1}^{K+1} b_k F_k(1) = 0, \quad \sum_{k=1}^{K+1} c_k F_k(1) = 0, \\ \sum_{k=1}^{K+1} d_k F_k(1) = 0, \quad \sum_{k=1}^{K+1} e_k F_k(1) = 0, \end{aligned} \right. \quad (14a)$$

hinged:

$$\left\{ \begin{aligned} \sum_{k=1}^{K+1} a_k F_k(1) = 0, \quad \sum_{k=1}^{K+1} b_k F_k(1) = 0, \\ \sum_{k=1}^{K+1} c_k F_k(1) = 0, \quad \sum_{k=1}^{K+1} e_k F_k(1) = 0, \\ \sum_{k=1}^{K+1} \left[d_k \left\{ \frac{F'_k(1)}{\Phi} + \frac{\nu F_k(1)}{\tan \Phi} \right\} + e_k \frac{\nu n F_k(1)}{\sin \Phi} \right] = 0, \end{aligned} \right. \quad (14b)$$

free:

$$\left\{ \begin{aligned} \sum_{k=1}^{K+1} \left[a_k \left\{ \frac{F'_k(1)}{\Phi} + \frac{\nu F_k(1)}{\tan \Phi} \right\} + b_k \frac{\nu n F_k(1)}{\sin \Phi} + c_k (1+\nu) F_k(1) \right] = 0 \\ \sum_{k=1}^{K+1} \left[-a_k \frac{n F_k(1)}{\sin \Phi} + b_k \left\{ \frac{F'_k(1)}{\Phi} - \frac{F_k(1)}{\tan \Phi} \right\} \right] = 0, \\ \sum_{k=1}^{K+1} \left[d_k \left\{ \frac{F'_k(1)}{\Phi} + \frac{\nu F_k(1)}{\tan \Phi} \right\} + e_k \frac{\nu n F_k(1)}{\sin \Phi} \right] = 0, \\ \sum_{k=1}^{K+1} \left[-d_k \frac{n F_k(1)}{\sin \Phi} + e_k \left\{ \frac{F'_k(1)}{\Phi} - \frac{F_k(1)}{\tan \Phi} \right\} \right] = 0, \\ \sum_{k=1}^{K+1} \left[-a_k F_k(1) + c_k \frac{F_k(1)}{\Phi} + d_k R F_k(1) \right] = 0. \end{aligned} \right. \quad (14c)$$

A boundary condition set out of Eqs. (14a)-(14c) can be rewritten in the matrix form,

$$[\mathbf{F}(n)]\{\delta\} + [\mathbf{G}(n)]\{\chi\} = \{0\} \quad (15)$$

where $\{0\}$ is a zero vector. Since $\{\chi\}$ in Eq. (15) can be expressed as

$$\{\chi\} = -[\mathbf{G}(n)]^{-1}[\mathbf{F}(n)]\{\delta\}, \quad (16)$$

Eq. (12) can be reformulated as

$$\begin{aligned} & \left([\mathbf{A}(n)] - [\mathbf{B}(n)][\mathbf{G}(n)]^{-1}[\mathbf{F}(n)] \right) \{\delta\} \\ & = \omega^2 \left([\mathbf{C}(n)] - [\mathbf{D}(n)][\mathbf{G}(n)]^{-1}[\mathbf{F}(n)] \right) \{\delta\}. \end{aligned} \quad (17)$$

The solution of Eq. (17) yields the estimates for the natural frequencies and corresponding expansion coefficients. Easy implementation of the boundary conditions is one of the merits of the present study. The procedure outlined in Eqs. (14)-(17) can be applied to the vibration analysis of spherical caps with the clamped, hinged and free boundary conditions.

3. Numerical examples

The algebraic problem of Eq. (17) is solved for the natural frequencies using Matlab. A convergence check of the natural frequencies of a clamped hemispherical shell for the axisymmetric mode ($n=0$) is performed and the computed frequency parameter $\Omega = \omega R \sqrt{\rho/E}$ is given in Table 1. The number of collocation points K ranges from 20 to 80. It is shown it requires less than $K=60$ for the lowest five natural frequencies to converge to three significant digits. The convergence is considerably slower than the Timoshenko beams [15] that had required less than $K=20$ for the lowest six natural frequencies to converge to six significant digits.

The computed frequencies are in excellent agreement with those of Kunieda [3]. Poisson's ratio and the shear correction factor are $\nu=0.3$ and $\kappa=5/6$ throughout the present study.

The present method is also proved for the asymmetric cases. The frequency parameter $\Omega = \omega R \sqrt{\rho(1-\nu^2)/E}$ of clamped and hinged hemispherical shells for the asymmetric modes ($n=1, 2, 3,$

Table 1. Convergence test of frequency parameter $\Omega = \omega R \sqrt{\rho/E}$ of axisymmetric modes of hemispherical shell vibrations ($\Phi = \pi/2$) with clamped boundary conditions for $R/h = 100$, $\nu = 0.3$ and $\kappa = 5/6$.

n	mode	present study				Kunieda [3]
		K=20	K=40	K=60	K=80	
0	1	0.7625	0.7618	0.7614	0.7614	0.760
	2	0.9408	0.9395	0.9387	0.9385	0.938
	3	0.9898	0.9872	0.9854	0.9851	0.984
	4	1.0332	1.0275	1.0238	1.0230	1.020
	5	1.0953	1.0836	1.0763	1.0750	1.071

Table 2. Comparison of frequency parameter $\Omega = \omega R \sqrt{\rho(1-\nu^2)}/E$ of asymmetric modes of hemispherical shell vibrations ($\Phi = \pi/2$) for $R/h = 100$, $\nu = 0.3$, $\kappa = 5/6$ and $K = 80$.

n	mode	clamped boundary conditions		hinged boundary conditions	
		present study	Singh Mirza [7]	present study	Singh Mirza [7]
1	1	0.5424	0.5424	0.5351	0.5345
	2	0.8527	0.8526	0.8449	0.8446
	3	0.9225	0.9211	0.9175	0.9162
	4	0.9586	0.9556	0.9527	0.9500
	5	1.0012	0.9961	0.9917	0.9870
2	1	0.8598	0.8598	0.8590	0.8590
	2	0.9219	0.9218	0.9218	0.9217
	3	0.9519	0.9517	0.9514	0.9511
	4	0.9837	0.9835	0.9787	0.9784
	5	1.0301	1.0307	1.0180	1.0182
3	1	0.9040	0.9041	0.9024	0.9024
	2	0.9439	0.9439	0.9426	0.9425
	3	0.9771	0.9772	0.9764	0.9763
	4	1.0171	1.0177	1.0167	1.0172
	5	1.0711	1.0732	1.0620	1.0633
4	1	0.9247	0.9248	0.9234	0.9234
	2	0.9589	0.9590	0.9577	0.9577
	3	0.9962	0.9966	0.9958	0.9960
	4	1.0443	1.0453	1.0432	1.0442
	5	1.1102	1.1137	1.0990	1.1013
5	1	0.9396	0.9397	0.9387	0.9387
	2	0.9740	0.9742	0.9733	0.9734
	3	1.0166	1.0170	1.0166	1.0169
	4	1.0738	1.0751	1.0701	1.0713
	5	1.1534	1.1583	1.1382	1.1413

Table 3. Frequency parameter $\Omega = \omega R \sqrt{\rho/E}$ of axisymmetric modes of hemispherical shells ($\Phi = \pi/2$) with free boundary conditions for $R/h = 100$, $\nu = 0.3$, $\kappa = 5/6$ and $K = 80$.

n	mode	present study	Chao et al [4]
0	1	0.8707	0.8705
	2	0.9531	0.9527
	3	0.9839	0.9862

4, 5) is given in Table 2 where the finite element solutions of Singh and Mirza [8] are also given for comparison, and where it is shown that the computed frequency parameters are practically identical to those of the finite element analysis in the lower modes and deviate slightly for the higher modes.

While there are numerous reports on the subject of the spherical shell vibrations with clamped and hinged boundary conditions only a limited number of solutions are available for the spherical shell vibrations with free boundary conditions. Studies on the asymmetric vibrations of spherical caps [6, 7, 8, 10,

Table 4. Frequency parameter $\Omega = \omega R \sqrt{\rho/E}$ for spherical caps with free boundary conditions for $R/h = 200$, $\nu = 0.3$, $\kappa = 5/6$ and $K = 80$.

Φ		n=0	n=1	n=2	n=3	n=4	n=5	n=6	n=7
$\pi/6$	1	0.9766	0.0119	0.0388	0.0853	0.1475	0.2236	0.3124	0.4130
	2	1.0170	0.9930	1.0103	1.0371	1.0773	1.1345	1.2113	1.3093
	3	1.1156	1.0527	1.1023	1.1768	1.2759	1.4002	1.5493	1.7219
	4	1.3359	1.2053	1.3127	1.4552	1.6255	1.8214	2.0410	2.2825
	5	1.7049	1.4967	1.6719	1.8857	2.1253	2.3882	2.6726	2.9769
$\pi/4$	1	0.9482	0.0063	0.0187	0.0423	0.0745	0.1147	0.1619	0.2158
	2	0.9879	0.9683	0.9820	0.9936	1.0060	1.0214	1.0415	1.0676
	3	1.0160	0.9994	1.0124	1.0312	1.0564	1.0894	1.1314	1.1832
	4	1.0706	1.0385	1.0644	1.1020	1.1501	1.2094	1.2803	1.3630
	5	1.1721	1.1142	1.1615	1.2262	1.3037	1.3941	1.4970	1.6120
$\pi/3$	1	0.9192	0.0047	0.0116	0.0272	0.0489	0.0762	0.1087	0.1460
	2	0.9731	0.9424	0.9627	0.9759	0.9860	0.9952	1.0050	1.0165
	3	0.9933	0.9817	0.9903	0.9996	1.0104	1.0237	1.0403	1.0608
	4	1.0155	1.0028	1.0130	1.0274	1.0457	1.0685	1.0965	1.1303
	5	1.0528	1.0319	1.0488	1.0731	1.1032	1.1395	1.1825	1.2325
$\pi/2$	1	0.8702	0.0028	0.0070	0.0183	0.0346	0.0552	0.0799	0.1083
	2	0.9503	0.8764	0.9165	0.9433	0.9602	0.9719	0.9808	0.9884
	3	0.9766	0.9512	0.9641	0.9741	0.9822	0.9895	0.9967	1.0044
	4	0.9908	0.9767	0.9833	0.9901	0.9971	1.0047	1.0135	1.0238
	5	1.0005	0.9916	0.9974	1.0048	1.0134	1.0236	1.0358	1.0502

Table 5. Frequency parameter $\Omega = \omega R \sqrt{\rho/E}$ for hemispherical shells with free boundary conditions for $R/h = 100$, $\nu = 0.3$, $\kappa = 5/6$ and $K = 80$.

Φ		n=0	n=1	n=2	n=3	n=4	n=5	n=6	n=7
$\pi/6$	1	0.9819	0.0263	0.0761	0.1649	0.2820	0.4244	0.5910	0.7816
	2	1.0873	1.0156	1.0682	1.1586	1.2925	1.4724	1.6973	1.9643
	3	1.4073	1.2092	1.3703	1.5940	1.8684	2.1880	2.5482	2.9452
	4	2.0168	1.6719	1.9652	2.3230	2.7250	3.1659	3.6421	4.1509
	5	2.8938	2.4192	2.8319	3.3078	3.8222	4.3708	4.9510	5.5609
$\pi/4$	1	0.9499	0.0122	0.0369	0.0824	0.1438	0.2190	0.3067	0.4061
	2	1.0018	0.9729	0.9940	1.0203	1.0566	1.1073	1.1753	1.2626
	3	1.0849	1.0327	1.0752	1.1383	1.2229	1.3304	1.4609	1.6139
	4	1.2658	1.1583	1.2489	1.3697	1.5161	1.6868	1.8802	2.0947
	5	1.5740	1.3996	1.5498	1.7335	1.9419	2.1725	2.4237	2.6940
$\pi/3$	1	0.9202	0.0070	0.0229	0.0532	0.0949	0.1466	0.2073	0.2760
	2	0.9780	0.9440	0.9666	0.9849	1.0035	1.0259	1.0546	1.0917
	3	1.0150	0.9922	1.0108	1.0362	1.0700	1.1141	1.1700	1.2386
	4	1.0838	1.0429	1.0776	1.1258	1.1873	1.2629	1.3529	1.4574
	5	1.2079	1.1363	1.1977	1.2779	1.3737	1.4848	1.6109	1.7511
$\pi/2$	1	0.8707	0.0037	0.0138	0.0360	0.0674	0.1066	0.1528	0.2055
	2	0.9531	0.8768	0.9174	0.9453	0.9645	0.9798	0.9943	1.0099
	3	0.9839	0.9536	0.9684	0.9822	0.9960	1.0116	1.0301	1.0529
	4	1.0019	0.9848	0.9967	1.0117	1.0301	1.0528	1.0808	1.1150
	5	1.0322	1.0134	1.0298	1.0521	1.0798	1.1138	1.1548	1.2032

12] do not show how the vibrations of spherical shells with free boundary conditions can be dealt with. In the pseudospectral method the free boundary condition of Eq. (14c) is merged into the collocated equations (12) so that the system Eq. (17) can be tailored

Table 6. Frequency parameter $\Omega = \omega R \sqrt{\rho/E}$ for hemispherical shells with free boundary conditions for $R/h = 50$, $\nu = 0.3$, $\kappa = 5/6$ and $K = 80$.

Φ		$n=0$	$n=1$	$n=2$	$n=3$	$n=4$	$n=5$	$n=6$	$n=7$
$\pi/6$	1	1.0018	0.0535	0.1481	0.3164	0.5380	0.8100	1.1306	1.4986
	2	1.3273	1.1021	1.2702	1.5434	1.9083	2.3528	2.8660	3.4391
	3	2.1887	1.6868	2.1024	2.6292	3.2300	3.8933	4.6113	5.3781
	4	3.5375	2.8090	2.8692	4.1682	4.9586	5.7994	6.6849	7.6106
	5	4.3539	3.3507	3.4371	4.3892	5.7126	6.9591	8.1688	9.3583
$\pi/4$	1	0.9546	0.0253	0.0722	0.1589	0.2737	0.4133	0.5761	0.7618
	2	1.0556	0.9905	1.0400	1.1194	1.2364	1.3950	1.5957	1.8362
	3	1.3200	1.1573	1.2925	1.4836	1.7219	2.0027	2.3218	2.6753
	4	1.8312	1.5428	1.7920	2.1007	2.4508	2.8370	3.2554	3.7032
	5	2.5767	2.1758	1.9891	2.9406	3.3867	3.8634	4.3679	4.8977
$\pi/3$	1	0.9230	0.0149	0.0450	0.1032	0.1816	0.2773	0.3885	0.5142
	2	0.9942	0.9497	0.9818	1.0194	1.0702	1.1397	1.2321	1.3496
	3	1.0981	1.0332	1.0884	1.1694	1.2773	1.4132	1.5765	1.7663
	4	1.3165	1.1892	1.3003	1.4473	1.6241	1.8288	2.0591	2.3132
	5	1.6756	1.4765	1.5730	1.8681	2.1105	2.3778	2.6676	2.9783
$\pi/2$	1	0.8723	0.0070	0.0272	0.0700	0.1292	0.2018	0.2862	0.3812
	2	0.9619	0.8780	0.9207	0.9534	0.9814	1.0109	1.0465	1.0917
	3	0.9975	0.9617	0.9848	1.0131	1.0487	1.0946	1.1531	1.2260
	4	1.0509	1.0150	1.0478	1.0928	1.1509	1.2237	1.3122	1.4169
	5	1.1535	1.0948	1.1490	1.2205	1.3081	1.4121	1.5325	1.6690

for the analysis with the free boundary conditions. Table 3 shows the frequency parameter $\Omega = \omega R \sqrt{\rho/E}$ for hemispherical shells with free boundary conditions for axisymmetric modes, which are compared with those of Chao et al. [4]. Tables 4-6 show the frequency parameter $\Omega = \omega R \sqrt{\rho/E}$ for spherical cap vibrations with free boundary conditions for the circumferential wave number ranging from $n = 0$ to $n = 7$ and for the spherical cap angle $\Phi = \pi/6, \pi/4, \pi/3$ and $\pi/2$. The thickness ratio varies from $R/h = 50$ to $R/h = 200$. The case with $n = 0$ stands for the axisymmetric vibration and the cases with $n \geq 1$ represent asymmetric vibration. As a whole, the frequency parameter of the asymmetric modes increases as n increase. The frequency parameter of the first mode of the asymmetric modes, however, is surprisingly lower than that of higher modes and the corresponding axisymmetric mode. It is also apparent that the frequency parameter tends to increase as the thickness of the shell increases.

4. Conclusions

The pseudospectral method is applied to the axisymmetric and asymmetric free vibration analysis of spherical caps. The equations of motion take the effects of transverse shear and rotary inertia into ac-

count. The displacements and the rotations are represented by Chebyshev polynomials in the colatitudinal direction and Fourier series expansions in the circumferential direction. Considering the symmetry and the antisymmetry of the solutions odd functions and even functions of Chebyshev polynomials are used alternatively as basis functions according to the circumferential wave number. The equations of motion are collocated to yield the system of equations that correspond to the circumferential wave number. Numerical examples are provided for clamped, hinged and free boundary conditions. The results show good agreement with those of the existing literature

Acknowledgment

This work was supported by 2008 Hongik University Research fund.

References

- [1] W. H. Hoppmann, Frequencies of vibration of shallow spherical shells, *Journal of Applied Mechanics* (1961), 305-307.
- [2] A. Kalnins, Effects of bending on vibrations of spherical shells, *Journal of Acoustical Society of America* 36 (1) (1964) 74-81.
- [3] H. Kunieda, Flexural axisymmetric free vibrations of a spherical dome: exact results and approximate solutions, *Journal of Sound and Vibration* 92 (1) (1984) 1-10.
- [4] C. C. Chao, T. P. Tung and Y. C. Chern, Axisymmetric free vibration of thick orthotropic hemispherical shells under various edge conditions, *Journal of Vibration and Acoustics* 113 (1) (1991) 152-159.
- [5] C. Prasad, On vibration of spherical shells, *Journal of Acoustical Society of America* 36 (3) (1964) 489-494.
- [6] M. S. Zarghamee and A. R. Robinson, A numerical method for analysis of free vibration of spherical shells, *AIAA Journal* 5 (7) (1967) 1256-1261.
- [7] Y. C. Wu and P. Heyliger, Free vibration of layered piezoelectric spherical caps, *Journal of Sound and Vibration* 245 (3) (2001) 527-544.
- [8] A. V. Singh and S. Mirza, Asymmetric modes and associated eigenvalues for spherical shells, *Journal of Pressure Vessel Technology* 107 (1) (1985) 77-82.
- [9] A. Tessler and L. Spiridigliozzi, Resolving membrane and shear locking phenomena in curved

- shear-deformable axisymmetric shell elements, *International Journal for numerical methods in engineering* 26 (1988) 1971-1086.
- [10] B. P. Gautham and N. Ganesan, Free vibration characteristics of isotropic and laminated orthotropic spherical shells, *Journal of Sound and Vibration* 204 (1) (1997) 17-40.
- [11] G. R. Buchanan and B. S. Rich, Effect of boundary conditions on free vibration of thick isotropic spherical shells, *Journal of Vibration and Control* 8 (3) (2002) 389-403.
- [12] S. C. Fan and M. H. Luah, Free vibration analysis of arbitrary thin shell structures by using spline finite element, *Journal of Sound and Vibration* 179 (5) (1995) 763-776.
- [13] J. Lee, Free vibration analysis of cylindrical helical springs by the pseudospectral method, *Journal of Sound and Vibration* 302 (1-2) (2007) 185-196.
- [14] W. Soedel, On the vibration of shells with Timoshenko-Mindlin type shear deflections and rotary inertia, *Journal of Sound and Vibration* 83 (1) (1982) 67-79.
- [15] J. Lee and W. W. Schultz, Eigenvalue analysis of Timoshenko beams and axisymmetric Mindlin plates by the pseudospectral method, *Journal of Sound and Vibration* 269 (3-5) (2004) 609-621.



Jinhee Lee received B.S. and M.S. degrees from Seoul National University and KAIST in 1982 and 1984, respectively. He received his Ph.D. degree from University of Michigan in 1992 and joined Dept. of Mechano-Informatics of Hongik

University in Choongnam, Korea. His research interests include inverse problems, pseudospectral method, vibration and dynamic systems.